ELSEVIER

Coordination Chemistry Reviews 228 (2002) 227–236

COORDINATION CHEMISTRY REVIEWS

www.elsevier.com/locate/ccr

Interactions of Al(III) with a neurofilament heptapeptide fragment: AcLysSerProValValGluGly

T. Kiss [a,b,*], M. Kilyén [b], A. Lakatos [b], F. Evanics [c], T. Körtvélyesi [d,f], Gy. Dombi [c], Zs. Majer [e], M. Hollósi [e]

[a] *Department of Inorganic and Analytical Chemistry, University of Szeged, PO Box 440, Szeged, Hungary*
[b] *Biocoordination Chemistry Research Group of the Hungarian Academy of Sciences, University of Szeged, PO Box 440, Szeged, Hungary*
[c] *Department of Pharmaceutical Analytical Chemistry, University of Szeged, PO Box 427, Szeged, Hungary*
[d] *Department of Biomedical Engineering, Boston University, Boston, MA 02215, USA*
[e] *Department of Organic Chemistry, Eotvos University, PO Box 32, Budapest, Hungary*
[f] *Department of Physical Chemistry, University of Szeged, PO Box 105, Szeged, Hungary*

Received 14 August 2001; accepted 12 February 2002

Contents

Abstract

The solution state of the neurotoxic Al(III) in biological systems is discussed briefly, and the importance of the Al(III)–peptide and Al(III)–protein interactions in the various neurodegeneration processes is emphasised and evaluated. The possible involvement of Al(III) in the formation of Alzheimer's disease marker senile plaques and neurofilament tangles is discussed in light of the solution speciation of the Al(III)–AcLysSerProValValGluGly system and the structural features of the complexes formed.

Keywords: Al(III)-complexes; Speciation; NMR; Molecular dynamics calculations

* Corresponding author. Tel.: +36-62-544-337; fax: +36-62-420-505.
E-mail address: tkiss@chem.u-szeged.hu (T. Kiss).

0010-8545/02/$ - see front matter
PII: S0010-8545(02)00073-5

1. Introduction

Aluminium has been recognised to be a neurotoxic element, but its aetiological role in Alzheimer's disease (AD) and other neurological disorders is rather controversial [1]. There seems to be no single unifying mechanism that can explain the wide variety of pathological, neurochemical and behavioural consequences of exposure to Al(III). It appears very likely, however, that Al(III) can strongly alter normal cellular metabolic pathways. As a strong Lewis acid and hard metal ion, Al(III) may react with numerous enzyme- and non-enzyme proteins, mostly through interactions with the negatively charged oxygen donor side-chain functional groups [2,3]. Although it has not been unambiguously clarified, Al(III) is almost certainly present at elevated concentration in the brain in many neurological disorders. Al(III) may occur both inside and outside neurons in the brain. There are several ways by which enhanced Al(III) levels may influence the structural or functional protein constituents of nerve cells. The neurotoxicity of Al(III) may stem from its promotion of the aggregation of phosphorylated neurofilament subunits, its catalysis of phosphorylation, or its inhibition of the dephosphorylation of tau protein, the main constituent of neurofibrillary tangles (NFTs). The other main form of neuronal degradation is the formation of senile plaques (SPs), which, like the tangles, are characteristic markers of AD. These amyloid plaques were found to accumulate Al(III). It is not clear, however, whether these metal ion binders behave only as a sink of metal ions, such as Al(III), or whether their formation is also induced or accelerated by Al(III). A further, and again rather unclear area is the possible effect of chelator molecules on these neurological disorders. Chelation is accepted therapy in cases involving Al(III) overload and there is evidence that desferrioxamine (DFO) and various pyridinone derivatives, for instance, can reduce the Al(III) level in the brain. As concerns the application of DFO in AD, there is a single paper from MacLachlan et al. [4], which reports that the sustained administration of DFO slowed down the progression of AD-type dementia. Their work has been criticised from many respects [5], but never repeated.

In 1995 the Vancouver Workshop on Aluminium Toxicity posed the following questions concerning the problem of whether the controversy of the role of Al(III) in AD can be resolved [6]:

1) Are there elevations of the concentration of Al in the brains of AD patients?
2) Is there a relationship between environmental exposure to Al(III), particularly in the drinking water, and an increased risk of AD?
3) Is treatment with DFO a potentially useful therapeutic approach, and to what extent might beneficial effects of DFO implicate Al(III) in the aetiology of AD?
4) Are there similarities between experimental animal studies and AD, particularly in the development of abnormal forms of tau protein seen in NFTs?
5) Does Al(III) promote deposition of the β-amyloid peptide in AD?
6) Does hyperaluminaemia associated with long-term haemodialysis treatment induce neurofibrillary degeneration?

Although these questions cannot be answered easily and unambiguously, it is surprising how little has been achieved in the past 5 years towards their clarification. After the mid-1990s, there was a rapid decline in intensity of the research relating to the role of Al(III) in the aetiology of AD. We believe that this was due in part to the relatively sparse X-ray crystallographic or NMR spectroscopic evidence indicative of the occurrence of Al(III) complexes of peptides and proteins involved in the formation of SPs and NFTs. The X-ray crystal structures of selected Al(III) compounds which may be of relevance for an understanding of Al(III) binding in biological contexts have been reviewed [7]. X-ray data on complexes of Al(III) with porphyrins and phthalocyanines are discussed in that review, but not a single Al(III) complex of a protein or peptide is mentioned. Another reason is the complexity of the coordination chemistry of Al(III), which complicates the planning of the experiments, from the selection of the Al compound to be applied to the evaluation of the results. The strong tendency of Al(III) to hydrolyse and its rather sluggish complexation kinetics cause severe difficulties as concerns an exact description of the solution state of Al(III) and its existing forms in biological fluids and tissues [8,9]. In an excellent review dedicated to amyloid fibrillogenesis [10], Al(III) is not listed as a risk factor of AD. Amyloid fibrils, including those constituting the SPs in AD, are suggested to be formed by a common self-assembly pathway. However, environmental factors (including temperature, ionic strength, pH and oxidation potential, but not metal ions) are mentioned as influencing protein unfolding, nucleation and protofibril elongation. Similarly, in the annual report of The American Alzheimer Association for 1999, Al(III) is again not mentioned at all [11].

2. Chemical forms of Al(III) in biological systems

The behaviour of Al(III) species in cells and biological fluids can be described in terms of four different forms: (i) free or mononuclear ions, (ii) low molecular mass complexes, (iii) reversible macromolecular complexes, and (iv) irreversible macromolecular complexes [12].

As a highly-charged small cation, Al^{3+} is readily hydrolysed in aqueous solution in the absence of competing ligands. Neutral solutions give a precipitate of $Al(OH)_3$ that redissolves with the formation of $[Al(OH)_4]^-$, the primary soluble Al(III) species at pH > 7 at μM levels of total Al(III). However, solutions which are supersaturated with respect to amorphous $Al(OH)_3$ are frequently formed.

Al^{3+} is a typical hard metal ion, and its most likely binding sites in biosystems are O donors, and especially negatively-charged O donors. Carboxylate, phenolate, catecholate and phosphate are among the strongest Al(III) binders. Biomolecules containing such functions may be involved in the uptake and transport processes of Al(III).

Al(III) interacts with a large number of peptides, proteins, glycoproteins, and carbohydrates. The Al(III)-binding potential of these bioligands may be characterised by pAl ($pAl = -\log[Al^{3+}]$), i.e. the negative logarithm of the free Al^{3+} concentration. pAl values are computed from the thermodynamic stability constants at known total concentrations of the metal ion and the ligand. The higher the pAl value, the higher the binding strength of the biomolecule. The data in Table 1 show that amino acids are weak binders, an oligopeptide is strong enough to prevent the precipitation of $Al(OH)_3$, while a protein with a specific donor group arrangement can be an extremely strong binder. The natural siderophore DFO is one of the strongest Al(III) binders known. Unfortunately, very little is known about the chemistry, binding strength and binding mode of its complexes with peptides and proteins. Al(III)-transferrin complexes have been relatively well characterised. In consequence of the lack of sufficient quantitative information, it is not easy to assess the biological relevance and possible biological roles of these interactions of Al(III).

Table 1
Most probable Al(III) complexes and pAl values at pH 7.4 and 25 °C [a]

Bioligand	Species present [b]	pAl [c]
Lactic acid	Metastable solution + $Al(OH)_3$ (s)	10.7
Oxalic acid	$Al_2(OH)_2L_4$ + $Al(OH)_3$ (s)	10.7
Catecholamines	AlL_3	12.5–13.4
Citric acid	$Al(LH_{-1})L$, $Al_3(LH_{-1})_3(OH)$	12.9
Hydroxide	Amorphous $Al(OH)_3$	10.7
Phosphate [d]	$Al(PO_4)_n(OH)_{3(1-n)}$ (s) (composition variable from $n = 0$–1)	11.4
Silicate [e]	$Al_2(OH)_4Si_2O_5$ (s)	12.6
Desferrioxamine	AlL	20.9
Phosphoserine (Ser(P))	AlL(OH), $Al(OH)_4$	10.8
2,3-dpg [f]	AlL, AlL(OH)	12.1
ATP	AlL_2, $AlL_2(OH)$	12.2
Amino acids	$Al(OH)_3$ (s)	10.7
Heptapeptide [g]	$AlL(OH)_2$	11.6
Transferrin	AlL	15.3

[a] Taken from Ref. [9,3].
[b] L is an abbreviation for ligand and (s) denotes a solid precipitate. For the citrate complexes, $H_{-1}L$ represents a coordinated citrate ligand in which the hydroxy group and all three carboxylate groups have been deprotonated. The overall charges on the complexes have been omitted.
[c] $pAl = -\log[Al^{3+}]$, calculated for 1 μM total Al^{3+} and 50 μM total ligand.
[d] 2 mM Total phosphate, typical of plasma.
[e] 5 μM Total $Si(OH)_4$, typical of plasma.
[f] 2,3-Diphosphoglyceric acid.
[g] See later text.

As regards irreversible macromolecular Al(III) complexes, Al(III) is a rather sluggish metal ion, but its practically irreversible binding in biological systems is nevertheless rather rare. It may occur, however, in molecular aggregates, when the exchange reactions of Al(III) are slowed down because of the formation of hydrolysed oxo or hydroxo-bridged Al clusters wrapped around by organic compounds. Al(III) accumulated in the brain in NFTs and SPs may represent such complexes. Again, the quantitative information available on these interactions is rather limited.

3. Interactions of Al(III) with oligopeptides

As mentioned above the involvement of Al(III) in AD is a somewhat controversial issue [6]. There are probably a majority who deny any connection between Al(III) and AD. In our view, Al(III) is certainly not a causative factor in AD, but it may be a risk factor as it can enhance SP and NFT formation [13,14]. It has been clearly demonstrated by CD and FTIR methods that Al(III) can interact with O donors, such as the Asp–COO^-, Glu–COO^-, Ser–OH, Thr–OH or Tyr–O^- fragments of β-amyloids or neurofibrillary proteins either via intramolecular complexation, causing conformational changes, or via intermolecular complex formation, linking peptide chains together through the carboxylates or phosphorylated Ser or Tyr sites. This leads to the aggregation of neuronal degradation products. CD and FTIR measurements have clearly indicated further that Al(III) induces conformational changes in the neurofilament proteins, yielding a high content of β-pleated sheet structure which facilitates aggregation. It has been assumed that Al(III) can interact both with the phosphorylated proteins, mostly via intermolecular bindings, and also with the nonphosphorylated proteins, via intramolecular binding, both forms of interaction resulting in some degree of aggregation [13].

The above-mentioned results led us to attempt to obtain quantitative equilibrium speciation and solution structural information concerning these interactions. Accordingly, we first studied the interactions of Al(III) with the building blocks of these compounds, i.e. amino

acids, such as Asp, Glu, Ser, etc. [15], and also with phosphorylated Ser and Tyr [16]. These amino acids are rather weak Al(III) binders; depending on the metal ion concentration, $Al(OH)_3$ precipitates at pH 3–4. Below this precipitation pH, monodentate COO^- coordination is the most obvious binding mode, but the NH_2 group can also take part in the coordination if it is surrounded by O^- donors, as in the case of Asp and Ser(P).

We continued with small peptide model systems, first the Al(III)–AspAsp and Al(III)–AspAspAsp systems. Depending on the Al(III) to ligand ratio, precipitation occurred at pH 5–6 in both systems. Monodentate and chelating coordination of the COO^- functions can be assumed in the acidic pH range, but, the early precipitation indicates that the terminal COO^- groups of Asp or Glu are not sufficiently strong in such a small peptide to keep Al(III) in solution and to prevent the precipitation of $Al(OH)_3$. To achieve this, a more specific arrangement of suitable side-chain donors is necessary.

We studied several synthetic fragments of mid-size neurofilament (NFM) peptides too. These were rich in Glu and Ser. The pentapeptides AcProGluValSerGlyNH_2 and HNProGluValSerGlyNH_2 had a protected C-terminus and a free or protected N-terminus. We found that the Al(III)-binding abilities of the peptides were stronger when they had a free ProNH function at the N-terminus. This is rather surprising as Al(III) is known [15,17] to have a low affinity for monodentate amines, and the N-terminal Pro-NH group is, therefore, not expected to be a strong binding site. As the C-terminal COO^- was blocked in both peptides, we would expect coordination via the side-chain Glu carboxylate and Ser alcoholate groups. Instead, coordination seems to be much more likely through the N-terminal donor groups.

4. The Al(III)–AcLysSerProValValGluGly heptapeptide system

This heptapeptide is also a synthetic NFM fragment and contains the repeating tetramer LysSerProVal, which is the recognition site of NFM [18]. CD [19] and FTIR [20] studies were carried out on such NFM peptides to detect any effects of Al(III) or other metal ions. It was found that the effect of Al(III) depended strongly on the solvent and the sequence of the peptides. In aqueous solution below pH 7, Al(III) did not give rise to any definite changes in the spectra. This shows that, even if it does bind to side-chain functionalities, Al(III) does not have an effect on the backbone conformation. However, in trifluorethanol, a solvent with unique solvating properties, Al(III) resulted in significant spectral effects, clearly indicating conformation changes in the peptide. In this work we used pH-potentiometric and multinuclear NMR techniques in order to detect any interactions between this peptide and Al(III) in aqueous solution.

4.1. Experimental

4.1.1. Materials

The peptide was synthesised on a BioSearch SAM II automated peptide synthesiser as described earlier [21], using the Fmoc–N-terminal protecting strategy and a modified M-BHA resin. The peptide was characterised by amino acid analysis, ^{1}H-NMR and positive ion FAB-MS [22]. The Al(III) stock solution was prepared from recrystallised $AlCl_3 \cdot 6H_2O$, and its concentration was determined gravimetrically through its oxinate. The stock solution contained 0.1 M HCl to prevent hydrolysis of the metal ion. The ionic strength of all solutions was adjusted to 0.20 M KCl and the temperature was 25.0 ± 0.1 °C.

4.1.2. Potentiometric measurements

The stability constants of the proton and the Al(III) complexes of the ligand were determined by pH-potentiometric titrations of 5 ml samples in the pH range 2–10 or until precipitation. The ligand concentration was 0.002 M and the metal ion to ligand ratio was 0:2, 1:2 or 2:2. In the consequence of the very small amount of ligand available, all three titrations were performed in the same sample; the solution titrated with 0.2 M KOH solution was reacidified to the starting pH, with a known amount of 0.2 M HCl acid solution. The pH was measured with a Molspin pH-meter with a Methrom combined glass electrode, which was calibrated for hydrogen ion concentration according to Irving et al. [23]. The concentration stability constants $\beta_{pqr} = [M_pL_qH_r]/[M]^p[L]^q[H]^r$ were calculated with the aid of the PSEQUAD computer program [24]. The stability constants used for the hydroxo species of Al(III) were taken from Ref. [25] and corrected to $I = 0.2$ by using the Davies equation: -5.49 for $[AlH_{-1}]^{2+}$, -13.54 for $[Al_3H_{-4}]^{5+}$, -108.6 for $[Al_{13}H_{-32}]^{7+}$ and -23.40 for $[AlH_{-4}]^-$.

4.1.3. NMR spectroscopy

^{1}H- and ^{13}C-NMR spectra were recorded at 25 °C with a Bruker Avance DRX400 spectrometer. Chemical shifts were referenced to the signal of TMS as an external standard. The samples were prepared in water containing 10% of D_2O to provide an NMR lock signal. The spectra of a 0.004 M solution of the peptide were measured at pH 4 and 7 in the absence and in the presence of an equimolar amount of the metal ion. The two-dimensional homocorrelated (^{1}H-COSY) and heterocorrelated (HSQC, HMBC) spectra were measured on a Bruker DRX500 spectrometer, using the standard Bruker microprogram.

4.1.4. Molecular modelling calculations

The structure of the AcLysSerProValValGluGly heptapeptide system was studied by molecular mechanics/molecular dynamics (MM/MD) methods in water with the application of implicit and explicit solvation models in the presence or in the absence of any counterions. The effects of the cations Na^+, Zn^{2+} and Al^{3+} on the structure were followed on the trajectory generated during 4 ns. Due to the lack of the necessary parameters the model of Al^{3+} ion was generated on the basis of the Mg^{2+} parameters. Na^+ served as a counterion to the negatively charged peptide molecule. Accordingly, the Na-peptide conformation may be considered as the conformation of the peptide free of metal ion coordination. Zn^{2+} was also studied, partly because of its similar nature to Al^{3+} (Zn^{2+} is not a real transition metal ion due to its filled d subshell), and partly because of its potential involvement of peptide aggregation processes [1].

4.1.5. Set-up of the MD simulation

The initial structure of AcLysSerProValValGluGly heptapeptide for the calculation of the structure with the lowest energy was built up as an extended structure by applying the TINKER package [26]. The structure was optimised with a convergence criterion of 0.001 kcal mol^{-1}, with the application of the AMBER-95 all-atom force field [27] and the GB/SA implicit solvation model [28]. By means of simulation annealing, 200 structures were generated by TINKER [26] with the following protocol: 10 ps thermal equilibration at 1500 K, followed by exponential cooling of the system to 50 K during 10 ps. The cut-off of the charge and the van der Waals interactions was 0.9 nm. The final structure was geometry optimised similarly to the initial one. This structure was used as the initial one for the next step. The steps were repeated 200 times. The structures of the lowest energy conformers were analysed. The lowest energy conformer was used as the initial structure in the isothermal molecular dynamics simulation.

The MD simulations were performed with the GROMACS program package [29], with a modified force field of GROMOS87, applying the united atom model. The ionizable residues were assigned formal charges appropriate to pH ~ 7 as Lys–NH_3^+, Glu–COO^- and the C-terminal Gly–COO^-. The peptide was placed in a cubic box with 3.25 nm sides and solvated with 1000 SPC/E water molecules. The box was large enough to contain the peptide molecule and 1.0 nm of solvent on all sides. The system was energy minimised with a criterion of 1000 kJ mol^{-1}. The water molecules at the lowest positive and/or negative potential energy positions were replaced by the counterions (a) Na^+, (b) Zn^{2+} and 1 Cl^- and (c) $Al^{3+}+2Cl^-$ in order to neutralise the system by means of GENION included in GROMACS [29]. The parameters for Al^{3+} were not available, and approximated values were, therefore, applied: all the parameters for Mg^{2+} were applied during the simulation except for the charge and molar mass, which were taken +3 and 26.9815, respectively. After the system had again been energy minimised, a 40 ps NVT restrained simulation was performed at 300 K.

The simulations were performed in the NPT ensemble with periodic box conditions at 300 K and 1 bar, using the weak coupling method [30], with relaxation times for the temperature and pressure of 0.1 and 0.5 ps, respectively. The dielectric constant used and the compressibility of water were 1.0 and 4.5 10^{-5} bar^{-1}, respectively. Peptide, solvent and counterions were independently coupled to the heat bath. The length of the time steps was 2 fs. The high order vibrational motions were eliminated by using LINCS [31] with a relative tolerance of 10^{-4}. For the SPC/E water molecules SETTLE [32] was applied, while the long-ranged electrostatic interactions were treated by the Particle Mesh Ewald (PME) method [33]. A distance of 0.9 nm was used for the electrostatic and van der Waals cut-offs. The trajectories of the 4000 ps molecular dynamics simulations were analysed starting at 20 ps.

4.1.6. Trajectory analysis

The total and potential energies, the root mean square deviations (RMSD) of the backbone (N–Cα–C) atoms relative to the initial structure, and fluctuation of the RMS of the backbone (N–Cα9–C) atoms were calculated. The distances of the cations (Na^+, Zn^{2+} and Al^{3+}) and the charged groups on the side chain were also analysed.

The secondary structures of the peptides were analysed by sampling the whole trajectory every 10 ps with the DSSP program [34]. The secondary structural elements were assigned via the definitions given in [35].

4.2. Results and discussion

4.2.1. Speciation

The N-protected heptapeptide AcLysSerProValValGluGly ($[H_2L]$, contains three protons that dissociate in the measurable pH range. That with the highest log K($[HL]^-$) value of 10.33 can be unambiguously ascribed to the Lys–NH_3^+ group. The acidities of the terminal COOH and the Glu–γ-COOH groups are comparable, and they lose two protons in parallel, overlapping processes in the acidic pH range. From a comparison of the macroscopic protonation constants (see Table 2) with those of other Glu-containing oligopeptides [36], the higher log K($[H_2L]$) value of 4.55 can be ascribed to the Glu carboxylate, and the other value, log K($[H_3L]^+$) = 3.39 to the terminal carboxylate, although these last two protons liberate in overlapping processes. The Ser–OH is very weakly

Table 2
Stability constants of proton (log K) and Al(III) complexes (log β) of the heptapeptide AcLysSerProValValGluGly at 25 °C and $I = 0.2$ M (KCl)

	log K/log β
log $K([HL]^-)$	10.33(5)
log $K([H_2L])$	4.55(3)
log $K([H_3L]^+)$	3.39(3)
$[AlLH_2]^{3+}$	17.11(8)
$[AlLH]^{2+}$	13.30(7)
$[AlL]^+$	9.36(6)
$[AlLH_{-1}]$	4.72(6)
$[AlLH_{-2}]^-$	−0.42(6)
Fitting (Δml) [a]	0.0032
Number of points	128

[a] The average difference between the experimental and the calculated titration curves, expressed in ml of the titrant.

acidic and does not dissociate in the measurable pH range.

The Al(III)–peptide system could be titrated up to pH ~ 10 without observable precipitation, although complexation slowed down in the pH range 7–9. In this pH range 10 min was not sufficient for pH equilibrium to be attained, and these points were, therefore, omitted from the speciation calculations. No measurements were made at a metal ion excess. Titration data were evaluated by the assumption of various mononuclear complexes in different protonation states. The best fit between the experimental and the calculated titration curves was obtained with the species and stability constants listed in Table 2. Complexes with stoichiometries other than 1:1 were rejected by the computer program. Species distribution curves are depicted in Fig. 1. The speciation diagram indicates that the interaction between Al(III) and the peptide molecule is fairly weak in the acidic pH range, as in equimolar solution only 20–30% of the ligand is bound to Al(III). The complex $[AlLH_2]^{3+}$ liberates four protons, with stepwise deprotonation constants of $pK([AlLH_2]^{3+}) = 3.81$, $pK([AlLH]^{2+}) = 3.94$, $pK([AlL]^+) = 4.64$ and $pK([AlLH_{-1}]) = 5.14$, which can be ascribed to deprotonation of the side-chain donor groups of the peptide and, in consequence of the hydrolytic tendency of Al(III), to dissociation of the coordinated water molecules around the metal ion. Complex formation becomes predominant only in the neutral pH range when the species $[AlLH_{-2}]^-$ is formed. It is worth mentioning that practically no binary hydroxo complexes of Al(III) are formed at a fourfold or higher excesses of the ligand in the pH range studied.

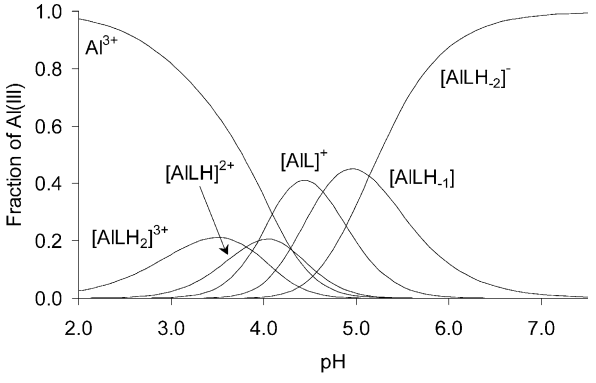

Fig. 1. Speciation curves for the complexes formed in the Al(III)–AcLysSerProValValGluGly system at a 1:4 metal ion to ligand ratio, with $c_{Al(III)} = 1$ mM.

4.2.2. NMR features of the Al(III)-ligand system

In order to specify the metal binding sites in the complexes formed, detailed NMR measurements were carried out. As a first step, the ^{1}H- and ^{13}C-NMR signals of the peptide were fully assigned by using the two-dimensional techniques listed in Section 4.1. The ^{1}H-NMR spectra of the peptide in the absence and in the presence of equimolar Al(III) are depicted in Figs. 2 and 3. The only singlet resonance at 2.03 ppm in the ^{1}H-NMR spectrum (Fig. 2a) can be unambiguously attributed to the methyl protons of the acetyl group from the N-terminus. This resonance served as our starting point in the signal assignment. The doublets of the methyl protons of the two Val appear at the highest fields (~ 1.1 ppm) as partly overlapping resonances (not shown in figure). The multiplets of the methylene groups of the peptide are present in a wide chemical shift range, between 1.3 and 4.0 ppm. The protons of the β-CH_2 group in Lys (1.81 and 1.72 ppm), Ser (3.84 and 3.90 ppm) and Glu (2.13 and 1.98 ppm) are magnetically non-equivalent, as often happens when the methylene group is situated near a chiral carbon. Similar splitting of the resonances can be observed for the two methylene groups (1 and 3) of the Pro ring, each of them giving rise to two multiplets, centred at 3.84 and 3.75 ppm, and 2.29 and 1.92 ppm, respectively. The signals of the

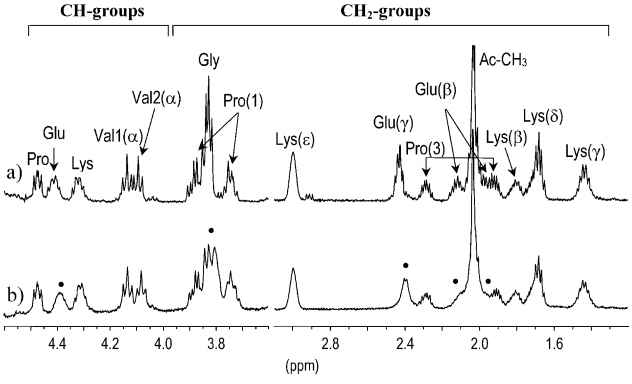

Fig. 2. ^{1}H-NMR spectra (δ range 0.5–4.5 ppm) of AcLysSerProValValGluGly at 4 mM at pH 4 (a) in the absence and (b) in the presence of 4 mM Al(III).

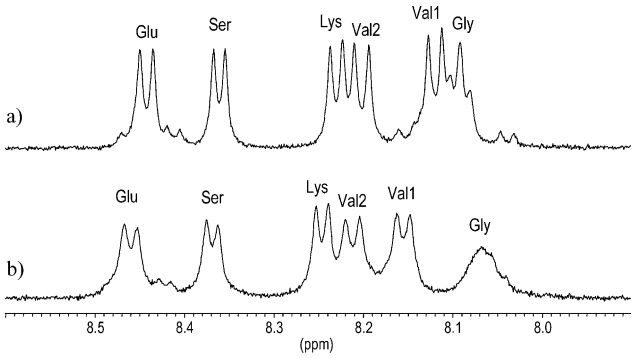

Fig. 3. ^{1}H-NMR spectra (amide δ range) of AcLysSerProValVal-GluGly at 4 mM at pH 4 (a) in the absence and (b) in the presence of 4 mM Al(III).

methyne protons of the peptide chain appear in the chemical shift range 4.0–4.5 ppm, except for that of Ser, which lies under the water signal. It has to be mentioned here that in Fig. 2, only the relatively well separated signals are marked; the peaks of the remaining groups occur as overlapping resonances in the chemical shift range 1.9–2.2 and 3.7–3.9 ppm. Their assignment and chemical shift values could be unambiguously obtained from the two-dimensional spectra but is difficult to indicate their assignment in the ^{1}H-NMR spectrum. At lower fields, between 8.0 and 8.5 ppm the spectrum reveals the resonances of the amide NH protons of the peptide bonds (Fig. 3a). The triplet at 8.09 ppm is due to Gly, while the remaining NH protons appear as doublets, since each of them is in the vicinity of a methyne group. The ^{1}H signal of the NH_2 group from the side-chain of Lys could not be detected, because of its rapid proton exchange with the solvent.

Fig. 2b and Fig. 3b depict the ^{1}H-NMR spectrum of the peptide at pH $\sim$4 in the presence of equimolar Al(III). Selective broadening of some signals (•) occurs as compared with the signals of the free ligand, indicating interactions between the peptide and the metal ion. The facts that neither separate resonances can be observed for the bound and unbound peptide, nor significant shifts in the position of the resonances occur (with exception of the amide protons), indicate that the rate of ligand exchange is roughly comparable with the ^{1}H-NMR timescale. In the chemical shift range of aliphatic protons, the resonances of Glu (β-CH_2, γ-CH_2 and CH groups) and of the CH_2 group of Gly are affected by the presence of Al(III) (Fig. 2b). At low fields (Fig. 3b), the signal of the amide–NH group of Gly exhibits an upfield shift and there is a considerable broadening as compared with the spectrum of the free peptide, while the signal of Val1 is shifted to higher chemical shift values without any change in its aspect. Slight downfield shifts of the other NH resonances can also be observed.

Similar results were obtained from the ^{13}C-NMR measurements. Fig. 4a and Fig. 5a show the J-MOD ^{13}C-NMR spectrum of the free ligand: the resonances of the CH and CH_3 groups appear as negative peaks, while the positive signals are those of the CH_2 and CO groups. In the aliphatic carbon region, the four peaks of the methyl carbons of the two Val show up at the highest fields, followed by the signal of the acetyl methyl group at 21.8 ppm (not shown in Fig. 4). The CH and CH_2 signals appear at higher chemical shift values, between 22 and 61 ppm. Their correct assignments are presented in Fig. 4a. In the carbonyl region (Fig. 5a), the resonances of the amide CO groups are present in a quite narrow range of 1.5 ppm, except that of Ser, which appears more separated at higher field: 170.2 ppm. The signals of the carboxylic groups of the C-terminal Gly and Glu can be located at lower fields: 175.2 and 178.1 ppm.

In the spectrum of the Al(III)-containing sample (Fig. 4b and Fig. 5b), the signals of the aliphatic C atoms of Glu (β-CH_2, γ-CH_2 and CH carbons) and Gly (CH_2 carbon) could not be detected; they probably fall into the baseline due to the their high linewidth. These resonances show up in the spectrum of the free peptide at 26.8, 30.8 and 53.2 ppm for Glu and 42.9 ppm for Gly. Similar broadening of the CO peaks of these two amino acids could be observed in the CO region of the same spectra (Fig. 5b).

This broadening of the above-mentioned signals in the ^{1}H- and ^{13}C-NMR spectra suggests the involvement of the corresponding amino acids in the coordination of Al(III), i.e. Al(III) is most probably bound at the C-terminus of the peptide through the terminal carboxylate group and the side-chain carboxylic function of Glu. Accordingly, it can be assumed that coordination

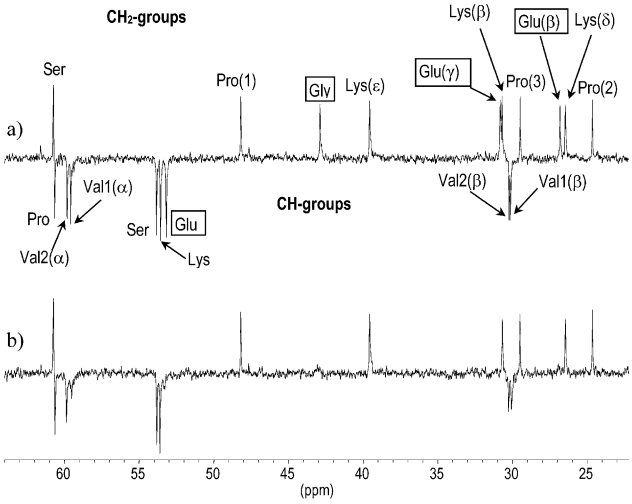

Fig. 4. ^{13}C-NMR spectra of AcLysSerProValValGluGly at 4 mM at pH 4 (a) in the absence and (b) in the presence of 4 mM Al(III). The symbols of the signals which disappear in the presence of Al(III) are placed in black boxes.

starts at the terminal COO^-, ($[AlLH_2]^{3+}$), and Al(III) then chelates through the terminal COO^- of the peptide and the side chain-COO^- of Glu, with participation of the central peptide carbonyl, through the formation of a joint chelate system ($[AlLH]^{2+}$), and then parallel overlapping deprotonation of the non-coordinating protonated amino donor and a coordinated water molecule subsequently takes place ($[AlL]^+$, $[AlLH_{-1}]$ and $[AlLH_{-2}]^-$).

The resonances of the two Val also suffer some smaller changes in the presence of Al(III) (see Figs. 3 and 4). This cannot be explained by the participation of these amino acids in binding of the metal ion, but more likely by some conformational changes of the peptide, induced by Al(III) (vide infra).

4.2.3. Molecular dynamics calculations

In order to confirm the proposed binding modes of Al(III) and also to examine whether Al(III) coordination results in any conformational change in the peptide backbone, molecular modelling calculations were carried out.

The optimal conformation of the free peptide was first calculated. Among the results of the simulated annealing calculations, five structures were found with an energy of less than -295.0 kcal mol^{-1} (AMBER-95 and GB/SA). The secondary structures of this peptide contain mainly an α-helix. In only one case was a turn structure found for SerProVal residues. The structure with the lowest energy is depicted in Fig. 6. The negative COO^- groups of Glu and the C-terminal Gly are localised on one side of the peptide, which can make binding of the cations possible. The distance between the protonated positively charged Lys and the negatively charged side-chain Glu is 0.5–0.7 nm; a bend/turn structure is stabilised in this small flexible peptide. The distance between the same Lys–NH_3^+ and the C-terminal Gly–

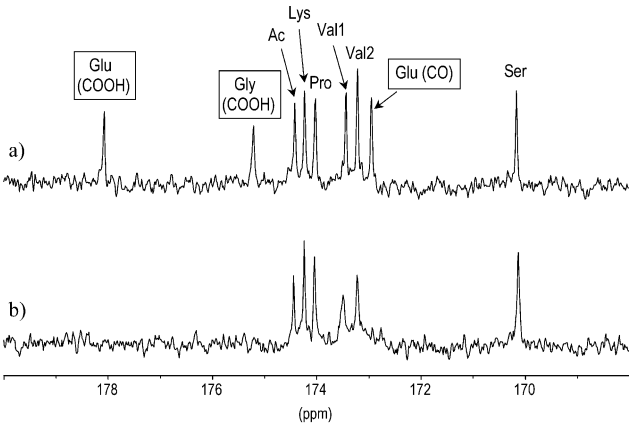

Fig. 5. ^{13}C-NMR spectra (carbonyl δ range) of AcLysSerProValVal-GluGly at 4 mM at pH 4 (a) in the absence and (b) in the presence of 4 mM Al(III). The symbols of the signals which disappear in the presence of Al(III) are placed in black boxes.

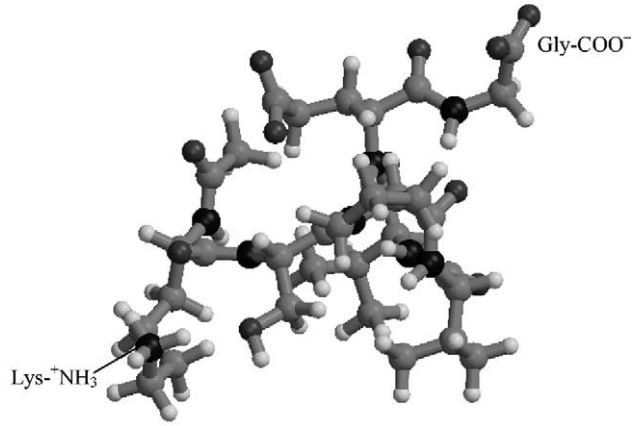

Fig. 6. Most stable structure of AcLysSerProValValGluGly obtained in the simulated annealing calculations (AMBER95 and GB/SA).

COO^- group is greater: it varies between 1.2 and 1.5 nm in all cases (Fig. 7).

The effects of the cations Na^+, Zn^{2+} and Al^{3+} on the structure of the peptide were also followed. In the evaluation of the data, we have to consider that the model for Al^{3+} is only an approximation. The change in the secondary structure during the molecular dynamics calculations at 20–4000 ps (see Fig. 8) relates to the destruction of the initial helical structure and the formation and stabilisation of bend (in the presence of Na^+) and turn (in the presence of Zn^{2+} and Al^{3+}) structures. The distances between the cations and the negatively charged COO^- functions varied significantly and revealed specific alterations, depending on the charge of the cations. With a great fluctuation, Na^+

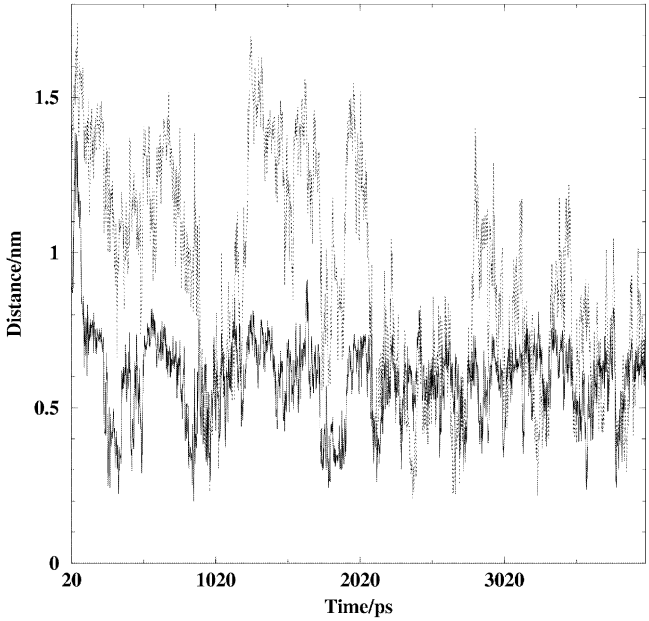

Fig. 7. Distance vs. simulation time plot: solid line, distance between Lys–NH_3^+ and Glu–COO^-; the dotted line, distance between Lys–NH_3^+ and Gly–COO^-.

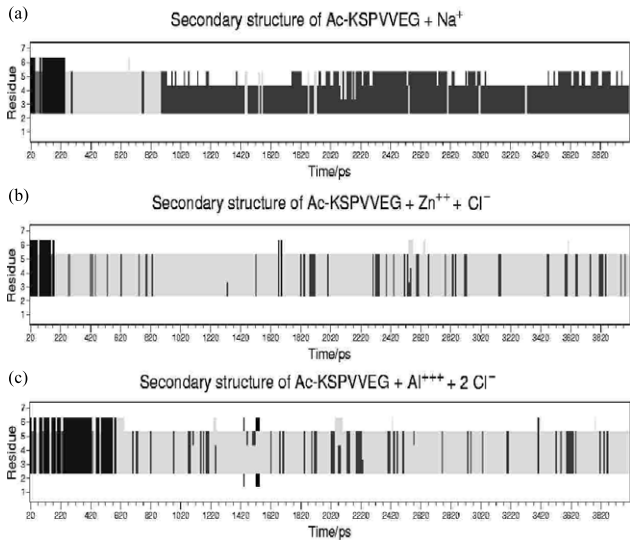

Fig. 8. Changes in the secondary structure during the simulation in the AcLysSerProValValGluGly+ (a) Na^+ (b) Zn^{2+} and (c) Al^{3+} systems: dark-grey: α-helical structure; grey: bend structure; and light-grey: turn structure.

was found to be closer to the C-terminal COO^- of the peptide than to the negative side chain of the Glu. The RMSD in the positions of the backbone atoms relative to the structure at 20 ps, was ca. 0.3 nm at the end of the simulation. The greatest root mean square fluctuation (S.D.) calculated for the individual backbone atomic/group positions was 0.15 nm for the residues 4 and 5 (Val, Val) during the simulation. The variations in the distances during the simulation were similar for Zn^{2+} and Al^{3+} too, but during ca. 50% (Zn^{2+}) and ca. 80% (Al^{3+}) of the simulation time the distance between the C-terminus and the cations is almost constant: 0.4–0.6 nm. In order to illustrate the effects of the cations on the peptide structure, the distances of Al^{3+} from the negatively charged Glu–COO^- and C-terminal Gly–COO^- as a function of time are depicted in Fig. 9. The fluctuation in the backbone atom distances (RMS) is significantly smaller in the simulation of the systems containing Zn^{2+} and Al^{3+} (0.07 nm for residues 4 and 5 (Val, Val) and 3 (Pro)).

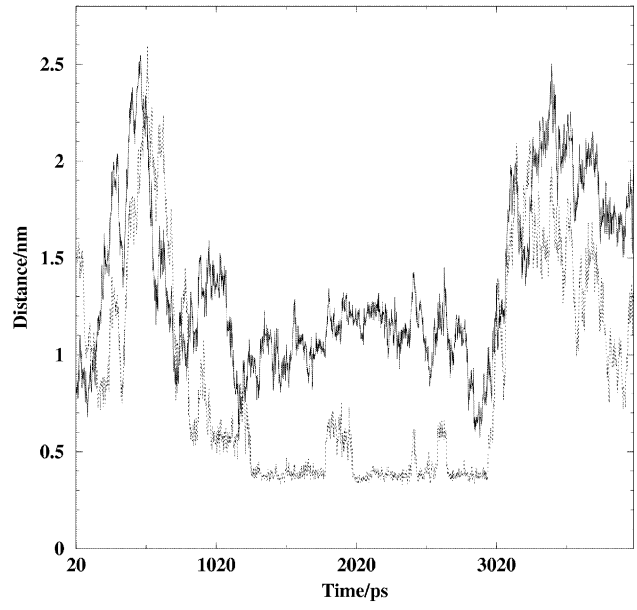

Fig. 9. Distance vs. simulation time plot: solid line, distance between Al^{3+} and Glu–COO^-; dotted line, distance between Al^{3+} and Gly–COO^-.

These molecular dynamics calculations suggest that the greater positive charge of the cations results in a more stable turn structure and a 'geometrically more stable' metal complex in the solution. They indicate favoured arrangements of the C-terminal COO^- and the side-chain COO^- of Glu for the chelation of Al(III). The average number of water molecules around Al^{3+} was found to be ca. six in a shell with a radius of 0.20 to 0.36 nm. The stability of the water shell around the Al^{3+} hindered the approach of the counterion in a shorter distance. This suggests that the interaction between the oppositely charged hydrated ions is mostly ionic character.

^{1}H-NMR measurements, similar as discussed above, were carried out at pH ~ 7 too. It is interesting, however, that at pH ~ 7 the two spectra (in the presence and absence of Al(III)) barely differ, and the direct coordination of Al(III) is, therefore, not confirmed. However, since no precipitation is observed in the solution, it is very likely that Al(III)-hydroxo species in some metastable state (which occurs fairly commonly in aqueous Al(III) solutions) form outer-sphere complexes through hydrogen-bonding with the hydrated oligopeptides.

5. Conclusions

To summarise the above studies, interactions between Al(III) and the heptapeptide AcLysSerProValVal-GluGly were unambiguously detected by pH-potentiometric and multinuclear NMR measurements in weakly acidic solutions. Molecular dynamics calculations confirmed the possible chelating binding of Al(III) to the negatively charged C-terminal Gly–COO^- and the side-chain Glu–COO^- groups. The coordination of Al(III) induced significant conformational changes from a more or less α-helical to a more turned conformation. These studies confirm that neurofilament non-phosphorylated peptides can bind Al(III), and this can trigger conformational changes which may result in an enhancement of aggregation processes of β-amyloids and NFTs. We intend to continue such investigations with similar oligopeptides, and also their phosphorylated derivatives, as interchain links between oligopeptides through Al(III) ions may play an even more important role in

the aggregation of neuropeptides than can intramolecular Al(III) binding. It may be assumed that binding of Al(III) at the carboxylate sites of neuropeptides influences the accessibility of Ser, Thr and Tyr phosphorylation sites via posttranslataional mechanisms, which may make the effects of Al(III) on brain peptides and proteins even more complex.

Acknowledgements

The work was carried out in the frame of a COST D8 collaboration and was supported by the Hungarian Research Fund (OTKA 23776/97) and the Hungarian Ministry of Education (FKFP 0013/97).

References

[1] C. Exley (Ed.),Aluminium and Alzheimer's Disease, Elsevier, Basel, 2001.
[2] R.B. Martin, Aluminium in Biology and Medicine, Wiley, Chichester, 1992, p. 5.
[3] T. Kiss, E. Farkas, Perspecitves on Bioinorganic Chemistry, 1996, p. 199.
[4] D.R.C. McLachlan, A.J. Dalton, T.P. Kruck, M.Y. Bell, W.L. Smith, W. Kalow, D.F. Andrews, Lancet 337 (1991) 1304.
[5] P. Davies, M.A. Weiner, D.R. Holleman, J.R. Goldstone, Lancet 338 (1991) 325.
[6] J. Savory, C. Exley, W.F. Forbes, Y. Huang, J.G. Joshi, T. Kruck, D.R.C. McLachlan, I. Wakayama, J. Toxicol. Environ. Health 48 (1996) 615.
[7] A.K. Powell, S.L. Heath, Coord. Chem. Rev. 149 (1996) 59.
[8] W.R. Harris, G. Berthon, J.P. Day, C. Exley, T.P. Flaten, W.F. Forbes, T. Kiss, C. Orvig, P.F. Zatta, J. Toxicol. Environ. Health 48 (1996) 543.
[9] W.R. Harris, Coord. Chem. Rev. 149 (1996) 347.
[10] J.C. Rochet, P.T. Lansbury, Jr., Curr. Opinion Struct. Biol. 10 (2000) 60.
[11] Report of the American Alzheimer Association, New York, 1999.
[12] T.L. Macdonald, R.B. Martin, Trends Biochem. Sci. 13 (1988) 15.
[13] M. Hollosi, L. Urge, A. Perczel, J. Kajtar, I. Teplan, L. Otvos, G.D. Fasman, J. Mol. Biol. 223 (1992) 673.
[14] C. Exley, N.C. Price, S.M. Kelly, J.D. Birchall, FEBS Lett. 324 (1993) 293.
[15] T. Kiss, I. Sóvagó, I. Tóth, A. Lakatos, R. Bertani, A. Tapparo, G. Bombi, R.B. Martin, J. Chem. Soc. Dalton Trans. (1997) 1967.
[16] E. Kiss, A. Lakatos, I. Bányai, T. Kiss, J. Inorg. Biochem. 69 (1998) 145.
[17] R.B. Martin, in: M. Nicolini, P.F. Zatta, B. Corain (Eds.), Aluminum in Chemistry, Biology and Medicine, Cortina International, Verona, 1991.
[18] V.M.-Y. Lee, L. Ötvös, Jr, M.J. Carden, M. Hollósi, B. Dietzschold, R.A. Lazzarini, Proc. Natl. Acad. Sci. USA 85 (1988) 1998.
[19] M. Hollósi, L. Ürge, A. Perczel, J. Kajtár, I. Teplán, L. Ötvös, Jr, G.D. Fasman, J. Mol. Biol. 223 (1992) 673.
[20] M. Hollósi, S. Holly, Zs. Majer, I. Laczkó, G.D. Fasman, Biopolymers 36 (1995) 381.
[21] Z.M. Shen, A. Perczel, M. Hollósi, I. Nagypál, G.D. Fasman, Biochemistry 33 (1994) 9627.
[22] L. Ötvös, I.A. Tangorem, K. Wroblewski, M. Hollósi, V.M.-Y. Lee, J. Chromatogr. 512 (1990) 265.
[23] H.M. Irving, M.G. Miles, L.D. Pettit, Anal. Chim. Acta 38 (1967) 475.
[24] L. Zékány, I. Nagypál, G. Peintler, PSEQUAD for Chemical Equilibria, Technical Software Distributions, Baltimore, 1991.
[25] L.O. Öhman, S. Sjöberg, Acta Chem. Scand. A36 (1982) 47.
[26] J.W. Ponder, TINKER, Software Tools for Molecular Design, Version 3.8, October 2000.
[27] W.D. Cornell, P. Cieplak, C.I. Bayly, I.R. Gould, K.M. Merz, Jr, D.M. Ferguson, D.C. Spellmeyer, T. Fox, J.W. Caldwell, P.A. Kollman, J. Am. Chem. Soc. 117 (1995) 5179.
[28] D. Qui, P.S. Shenkin, F.P. Hollinger, W.C. Still, J. Phys. Chem. A 101 (1997) 3005.
[29] (a) D. van der Spoel, A.R. van Buuren, E. Apol, P.J. Meulenhoff, D.P. Tieleman, A.L.T.M. Sijbers, R. van Drunen, H.J.C. Berendsen, GROMACS User Manual, University of Gronongen, 1996.;
(b) H.J.C. Berendsen, D. van der Spoel, R. van Drunen, Comp. Phys. Commun. 91 (1995) 43.
[30] H.J.C. Berendsen, J.P.M. Postma, A. DiNola, J.R. Haak, J. Chem. Phys. 81 (1984) 3684.
[31] B. Hess, H. Bekker, H.J.C. Berendsen, J.D.E.M. Fraaije, J. Comp. Chem. 18 (1997) 1463.
[32] J.P. Ryckaert, G. Ciccotti, H.J.C. Berendsen, J. Comp. Phys. 23 (1977) 327.
[33] (a) T. Darden, D. York, L. Pedersen, J. Chem. Phys. 98 (1993) 10089;
(b) U. Essmann, L. Perera, M.L. Berkowitz, T. Darden, H. Lee, L.G.A. Pedersen, J. Chem. Phys. 103 (1995) 8577.
[34] C.S. Kabsch, Biopolymers 22 (1983) 2577.
[35] T. Kortvelyesi, R.F. Murphy, S. Lovas, J. Biomol. Struct. Dyn. 17 (1999) 393.
[36] L.D. Pettit, H.K.J. Powell, The IUPAC Stability Constant Database, Academic Software and IUPAC, Royal Society of Chemistry, London, 1992–1997.